Freshwater Forcing of Atlantic Meridional Overturning Circulation Revisited

Feng He[*1], Peter U. Clark[2,3], Anders E. Carlson[4]

1. Center for Climatic Research, Nelson Institute for Environmental Studies, University of Wisconsin-Madison, Madison, WI 53706, USA

2. College of Earth, Ocean, and Atmospheric Sciences, Oregon State University, Corvallis, OR 97331, USA

3. School of Geography and Environmental Sciences, University of Ulster, Coleraine, Northern Ireland BT52 1SA, UK

4. Oregon Glaciers Institute, Corvallis, OR 97330, USA

* To whom correspondence should be addressed: fenghe@wisc.edu

Freshwater (FW) forcing is widely identified as the dominant mechanism causing reductions of the Atlantic Meridional Overturning Circulation (AMOC), a climate tipping point that led to past abrupt millennial-scale climate changes. However, the AMOC response to FW forcing has not been rigorously assessed due to the lack of long-term AMOC observations and uncertainties of sea-level rise and ice-sheet melt needed to infer past FW forcing. Here we show a muted AMOC response to FW forcing – ~50-m sea-level rise from the final deglaciation of Northern Hemisphere ice sheets – in the early-to-middle Holocene ~11,700-6,000 years ago. Including this muted AMOC response in a transient simulation of the Holocene with an ocean-atmosphere climate model improves agreement between simulated and proxy temperatures of the past 21,000 years. This demonstrates that the AMOC may not be as sensitive to FW fluxes and Arctic freshening as is currently projected for the end of the 21st century.

Pre-industrial climate evolution of the past 21,000 years indicates that global climate change was paced by Earth's orbital variations and driven mainly by abrupt changes in the Atlantic Meridional Overturning Circulation (AMOC)[1-3] and more-gradual changes in atmospheric CO_2[4,5]. A future disruption of the AMOC[6] could lead to drying of the Amazon rainforest, disruption of the Asian monsoon[7], rapid sea-level rise on the northeast coast of the United States[8], and widespread cessation of crop production in Europe[9]. Indirect assessments of AMOC trends from historical records are inconclusive, with an estimated 15% weakening since the mid-twentieth century based on sea surface temperature (SST) observations[10] and no change in the AMOC state since 1990s based on hydrographic data[11]. Continuous measurements of the AMOC started in 2004 with the Rapid Climate Change-Meridional Overturning Circulation and Heatflux Array (RAPID) program at 26.5ºN, which show that the AMOC weakened between 2004 and 2012 with a recovery since 2012[12]. Future projections of the AMOC with climate model simulations under high emission scenarios suggest a best estimate of 34-45% weakening of the AMOC during the 21st century[13,14] with surface warming and increased freshwater (FW) fluxes to the Arctic and North Atlantic Oceans from runoff and precipitation as well as melting of Arctic sea ice and the Greenland ice sheet[15-17]. However, it remains unclear whether the simulated AMOC reduction from global warming is more responsive to changes in surface heat fluxes or FW flux[15] since surface heat flux induces both surface warming and the melting of the Arctic sea ice with liquid FW exports to the North Atlantic Ocean[16], while FW-forcing-only experiments show that an enhanced hydrological cycle[18] and modest increases in FW fluxes projected from Greenland ice-sheet melting[13,17] can still weaken the AMOC.

While theoretical understanding of the AMOC response to FW forcing is reasonably well established[19], several issues regarding model design and implementation suggest that further evaluation of this relationship is warranted. For example, a recent study based on hydrographic data suggests a much more stable AMOC than previously thought due to a higher decoupling between the AMOC and ocean interior property fields[11]. Conversely, another study argues that climate models overestimate AMOC stability due to incorrect net-FW transport in the Atlantic Ocean[20], and that an AMOC collapse (~67% reduction) in response to global warming may occur by 2300 after correcting these biases with flux adjustments in the model[21], with the caveat that a model that correctly simulates surface density does not necessarily correctly simulate stability[22]. Another issue is the application of FW forcing to regions of deep water formation[23]. This includes concerns of correctly producing FW export from the Arctic to the North Atlantic Ocean through boundary currents in low-resolution ocean models[24] as well as the time scale and rate of FW forcing that affect the accumulated FW forcing to regions of deep water formation[25,26], but previous eddy-permitting ocean simulations (1/6º resolution) with realistic boundary currents show that AMOC reduces by ~30% with 1-year FW forcing from the Arctic[24]. Further issues include whether climate models form deep water in the correct region[27] and properly export FW from the subpolar gyre to the subtropical gyre through the Canary Current[28]. Finally, we note that multi-model ensemble in Coupled Model Intercomparison Project Phase 6 (CMIP6) show that model resolution in itself does not impact the projected AMOC decline at the end of 21st century[14,29] and recent studies with eddy-permitting coupled ocean-atmosphere (1/4º resolution) models[26] have identified similar rates and magnitudes of AMOC weakening to a 0.1 Sv FW forcing found in traditional non-eddy-permitting models.

Paleoclimate data synthesis

Much of the debate on the response of the AMOC to FW forcing reflects the lack of long-term observations of the AMOC and FW fluxes that could be used to validate models[10-12]. In this regard, the early-to-middle Holocene from ~11,700 to 6,000 years ago (11.7-6.0 ka) provides an opportunity to assess this issue due to well-constrained reconstructions of the AMOC and FW fluxes. In particular, global mean sea level rose ~60 m during this interval, with ~50 m of that rise derived from the final deglaciation of Northern Hemisphere ice sheets (Fig. 1c)[30-32]. This ice-sheet melting resulted in a sustained FW flux of ~0.1 Sv (1 Sv = 10^6 m^3 s^{-1}) to the Arctic and North Atlantic Oceans[33-36], which is similar to the distribution and amount (0.07-0.12 Sv) of projected runoff and precipitation minus evaporation (P-E) associated with future global warming[37,38]. In addition, after the opening of the Bering Strait following the Younger Dryas cold interval[39], FW transport from the Pacific Ocean to the Arctic Ocean increased and reached the modern day level of ~0.08 Sv[38] around 6 ka associated with the ~60 m sea-level rise during this interval. Climate model simulations show that a sustained flux of ~0.10-0.18 Sv should have caused a significant reduction in, if not a collapse of, the AMOC[14,18,26].

However, two independent proxies that provide kinematic reconstructions of the AMOC during the early-to-middle Holocene indicate little response to this FW forcing[40-42]. Instead, the $^{231}Pa/^{230}Th$ proxy from multiple Atlantic cores[40,43] as well as the $\delta^{18}O$ record from the Florida Straits[41] suggest the AMOC strengthened before ~9 ka and remained at a strength similar to the late Holocene between 9 ka and 6 ka (Fig. 1b). Furthermore, with the exception of the century-long 8,200-yr cold event[44], and perhaps two other similarly short-lived cold events[45,46], reconstructed Holocene Greenland surface temperatures show no signal of an AMOC-induced surface cooling such as the late-Pleistocene Younger Dryas cold period[47] (Fig. 1a). Instead, Greenland temperatures warmed during the early Holocene and remained at the level similar to the late Holocene between 9 ka and 6 ka in parallel with the AMOC changes suggested by the kinematic proxies[40,42] (Fig. 1). Having a sustained FW flux of ~0.10-0.18 Sv discharged into the

North Atlantic and Arctic Oceans from 11.7-6.0 ka in association with with little or no slowdown of the AMOC and associated cooling of North Atlantic climate constitutes a fundamental challenge to the paradigm of FW forcing of the AMOC, which we refer to as the "Holocene Meltwater-AMOC Paradox" (HMAP).

Transient Holocene simulations

We next illustrate how overestimation of AMOC sensitivity to FW forcing might cause temperature biases in future projections by comparing two transient simulations of the Holocene with and without FW forcing using the Community Climate System Model version 3 (CCSM3), a coupled ocean-atmosphere climate model of the US National Center for Atmospheric Research. We compare the surface temperature from the two simulations with three regional proxy temperature stacks from Greenland, Antarctica, and the Eastern Atlantic Ocean and Mediterranean Sea area that are known to be strongly influenced by changes in the AMOC (Fig. 2 and Extended Data Figs. 1-5; see Methods for further details).

The original TraCE-21K simulation (herein TraCE-21K-I) was forced by Earth's orbital variations, greenhouse gases, ice-sheet variations, and FW forcing[48,49]. Due to large uncertainties of geologic reconstructions of FW forcing before Bølling warming (~14.7 ka), the FW scheme in TraCE-21K-I was designed to reproduce changes in the AMOC as suggested by proxies between the Last Glacial Maximum (~21 ka) and onset of the Bølling warming, followed by a switch to a geologic reconstruction of FW forcing after the onset of Bølling warming[33-36,49]. For the Holocene, contributions to the FW forcing include the sustained ~0.1 Sv meltwater flux from Northern Hemisphere ice sheets to the Arctic and North Atlantic Ocean in the early-to-middle Holocene (Extended Data Figs. 6-7, Supplementary Table 2) and continuous inflow of fresher North Pacific water to the Arctic and North Atlantic Oceans after the opening of Bering Strait[49].

The simulated AMOC exhibits good agreement, by design, with proxy reconstructions of the AMOC through the onset of Bølling warming (21.0-14.5 ka) in TraCE-21K-I, with a strong AMOC reduction during the Oldest Dryas[48] (Fig. 2a). However, under the FW forcing during the Holocene, the AMOC never recovers to the strength suggested by the proxies, being weakest during the period of the HMAP and remaining weak in response to Bering Strait throughflow[49] in the late Holocene.

Global and hemispheric climate evolution simulated by TraCE-21K-I was in good agreement with global and regional proxy temperature stacks up to and including the onset of Bølling warming[4,5,48]. However, as with the AMOC, this agreement subsequently breaks down (Fig. 2). In particular, during the period of the HMAP, there is a clear mismatch between the proxy and modeled regional temperature stacks (Fig. 2 b-d and Extended Data Fig. 5), with a >8ºC cold bias in central Greenland, a >3ºC cold bias in the Eastern Atlantic Ocean and Mediterranean Sea, and an ~2ºC warm bias over Antarctica relative to the proxy records. The sign and amplitude of the simulated temperature biases reflects a bipolar seesaw response[18,48] to the weaker simulated AMOC during the early Holocene (Fig. 2a), which could also produce large biases in tropical precipitation and the global monsoons[7]. Similar temperature-AMOC biases during the early Holocene were also found in transient simulations of the early Holocene from the Loch-Vecode-Ecbilt-Clio-Agism Model (LOVECLIM) and the Fast Met Office/UK Universities Simulator (FAMOUS) model[50,51].

We reran TraCE-21K following the onset of Bølling warming (herein TraCE-21K-II) with the same climatic forcing as in TraCE-21K-I but with no FW fluxes during the Bølling-Allerød interstadial (~14.7 ka – 12.9 ka) and throughout the Holocene (Methods). In contrast to the TraCE-21K-I simulation with Holocene FW forcing, the modeled AMOC in TraCE-21K-II is in better agreement with proxy Holocene AMOC kinematic reconstructions (Fig. 2a). This includes a two-phase recovery suggested by the highest resolution reconstruction from the Florida Straits (blue in Fig. 1b)[41] involving an initial abrupt increase of the modeled AMOC after the end of FW forcing that was prescribed to cause the AMOC reduction during the Younger Dryas (Methods) followed by a further increase to full Holocene rates at ~9 ka (Fig. 2a). Ref.[52] attributed this two-phase AMOC recovery to an initial increase in deep water formation largely in the North Atlantic subpolar gyre and Irminger Sea regions followed by an abrupt increase of the AMOC when a density threshold is crossed in the Nordic Seas. In addition, the two-phase recovery of the AMOC is responsible for the temperature over Greenland and Eastern Atlantic Ocean/Mediterranean Sea reaching Holocene levels at ~9 ka (Fig 2b, c). Nevertheless, the model does not reproduce the transient temperature evolution during the two-phase recovery in the regional proxy temperature stacks due to the lack of understanding of the physical processes from changes in insolation, ice sheets and atmospheric greenhouse-gas concentrations that are responsible for transient AMOC changes on centennial time scales, although the changes in the latter two forcings during the Holocene likely had a small or negligible effect on the AMOC[13,51,53].

The more-realistic simulation of the AMOC after the two-phase recovery substantially improves the agreement between simulated temperatures in TraCE-21K-II and proxy temperatures (Fig. 2 b-d, Extended Data Fig. 5), largely removing the bias of the bipolar seesaw response due to the Holocene AMOC reduction in TraCE-21K-I (Fig. 3). Specifically, the cold bias of >8^{o}C over Greenland and >3^{o}C over the Eastern Atlantic Ocean/Mediterranean Sea in the TraCE-21K-I simulation during the period of the HMAP is reduced by ~80% and ~60%, respectively (Fig. 2b, 2c and Extended Data Fig.5). There is also an ~80% reduction of the warm bias over Antarctica due to the enhanced northward heat transport from the AMOC in TraCE-21K-II (Fig. 2d and Extended Data Fig. 5).

Implications for past climate changes

The successful transient simulation of the Holocene without FW forcing in TraCE-21K-II supports our inferences from the proxy data synthesis of the muted AMOC response to FW forcing in the Holocene. In addition, prior to the onset of Bølling warming, TraCE-21K-I simulated reasonable surface climate changes using a FW scheme designed to reproduce proxy-based AMOC changes[48], suggesting that prescribing the reconstructed AMOC instead of reconstructed FW forcing could improve the surface climate simulation of the Holocene and likely other past climate changes. Recent assessments of several proxy-based AMOC reconstructions during the last deglaciation concluded that they show coherent and robust changes during Heinrich event 1 and the Younger Dryas[41,43]. Nevertheless, these proxy signals can be modulated by other processes[54,55], and further work will be needed to reduce remaining uncertainties in the reconstructed AMOC changes if they are to be used as the target for prescribing the AMOC in model simulations.

In addition to the possible decoupling between the AMOC and ocean interior properties[11], a key issue likely contributing to the HMAP concerns how the meltwater from Northern Hemisphere ice sheets is distributed to sites of deep-water formation[23]. Much of the 0.1 Sv meltwater flux from retreating Northern Hemisphere ice sheets, however, entered the oceans along 1000's of kilometers of coastline bordering those oceans. For example, an estimated 0.02 Sv from the northern Laurentide ice sheet entered the Arctic Ocean along ~2,000 km of coastline during the early Holocene[34] which, if evenly distributed, corresponds to 0.0001 Sv per 10 km. Such small, local fluxes would likely be trapped along the coastline and quickly mixed by tides, wind forcing, and local circulation, and thus unlikely be uniformly spread over sites of North Atlantic deep-water formation.

One question raised by the HMAP is whether the sensitivity of the AMOC to FW forcing differed during the last deglaciation. Unfortunately, however, this question cannot be currently addressed because of the large uncertainties in the FW forcing during the last deglaciation which led to the strategy used by TraCE-21K-I of prescribing FW forcing to cause changes in the AMOC consistent with proxy reconstructions between the Last Glacial Maximum (~21 ka) and onset of the Bølling warming[48,49]. Whether that FW forcing is realistic and how much of the deglacial AMOC variability may have been associated with other forcings (e.g., ice-sheet orography, insolation) thus remains unclear[51].

Another question raised by the HMAP is whether the cold bias associated with a reduced AMOC in TraCE-21K-I and other transient Holocene simulations[50] reduced the modeled expression of a Holocene climate optimum around 9,000 to 5,000 years ago[56] that has been documented extensively in proxy records[57,58]. We find that the new transient Holocene simulation in TraCE-21K-II exhibits a brief climate optimum at ~9 ka (Extended Data Figs. 8-9) after removing the cold bias in the North Atlantic region in TraCE-21K-I during the HMAP, suggesting the missing Holocene climate optimum in TraCE-21K-I may in part be due to the cold bias from overestimation of AMOC sensitivity to FW forcing during the HMAP. For the late Holocene temperature conundrum[59], the lack of a cooling trend in TraCE-21K-I has been attributed to the underestimation of Arctic sea ice sensitivity to orbital forcing[60] and the lack of anthropogenic forcing from the Holocene deforestation in transient Holocene simulations[61].

Implications for future projections

Although the HMAP raises questions about the overestimation of AMOC sensitivity to FW forcing in current climate models, we emphasize that it does not challenge the role of the AMOC in causing abrupt climate changes in the past and potentially in the future. For instance, although the source and magnitude of FW forcing required to slow the AMOC during the Younger Dryas cold interval is still debated[62,63], the abrupt decrease of the AMOC during the Younger Dryas is widely accepted as the primary cause of the associated cooling (Fig. 2)[3,64]. We draw an analogy to atmospheric CO_2 whereby its role in causing past climate change is clear while at the same time there are large uncertainties in our understanding of the physical and biogeochemical processes and feedbacks that caused lower CO_2 during the Last Glacial Maximum and its subsequent increase[65]. Models thus prescribe CO_2 as a forcing of past climate changes using concentrations from ice-core records, whereas the simulated future emission-driven CO_2 changes using carbon-cycle models are regarded as uncertain[66]. For the same reason, we suggest that until the HMAP is resolved, any simulated future AMOC changes from FW forcing and associated temperature, precipitation and regional sea level changes should be viewed with caution (Fig. 3). In particular, having a stable AMOC in the face of sustained and large ~0.10 FW fluxes from ice-sheet melting and ~0.08 Sv from Bering Strait opening during the HMAP suggests that current projections of AMOC decline in the 21st century[14,66] from projected increase of runoff and P-E[37,38] as well as the FW exports to the North Atlantic Ocean as the result of the melting of Arctic sea ice from surface warming[16] may be overestimated, which precludes their use for assessing the likelihood of abrupt AMOC changes in the 21st century. As the projected increase of FW input into the Arctic at the end of the 21st century reaches a similar level of ~0.1 Sv FW forcing (~0.05 Sv from runoff, ~0.015 Sv from P-E[38], and 0.02-0.04 Sv from melting of the Greenland ice sheet[17,67-69]) as that associated with early Holocene ice-sheet melting, we conclude that there is an urgent need to assess whether AMOC sensitivity to FW forcing is overestimated in current climate models and investigate alternative mechanisms for past AMOC disruptions in both glacial and interglacial periods and incorporate these mechanisms in climate models for future projections.

Acknowledgments We thank J. D. Shakun and C. Buizert for fruitful discussions, and J. Lynch-Stieglitz for providing the AMOC data at the Florida Straits. This work was funded by the US National Science Foundation (NSF) through grant numbers AGS-1502990 and AGS-1602771 (to F.H.), AGS-1503032 (to P.U.C.), OPP-1936880 (to A.E.C. and F.H.); the Climate, People, and the Environment Program (to F.H.); and the NOAA Climate and Global Change Postdoctoral Fellowship program (to F.H.), administered by the University Corporation for Atmospheric Research. Support for this research was also provided by the University of Wisconsin-Madison Office of the Vice Chancellor for Research and Graduate Education with funding from the Wisconsin Alumni Research Foundation. This research used resources of the Oak Ridge Leadership Computing Facility at the Oak Ridge National Laboratory, which is supported by the Office of Science of the U.S. Department of Energy under Contract No. DE-AC05-00OR22725.

Author contributions F.H. designed and performed the research with inputs from P.U.C. and A.E.C.; F.H. led the writing of the manuscript with inputs from P.U.C. and A.E.C.; all authors discussed the results and contributed towards improving the final manuscript.

Competing interests The authors declare no competing interests.

Additional information

Supplementary information is available for this paper.

Correspondence and requests for materials should be addressed to F.H.

Peer review information Nature thanks (anonymous) reviewer(s) for their contribution to the peer review of this work.

Reprints and permissions information is available at http://www.nature.com/reprints.

Figure Captions

Fig. 1. Holocene Meltwater-AMOC Paradox. a, *Composite of temperature reconstruction over the central Greenland based on $\delta^{15}N$ for 22–10 ka at GISP2, NGRIP and NEEM site[47] and $\delta^{18}O$ for 10–0 ka at GIPS2 site[70].* ***b-c,*** *AMOC (**b**) and sea-level rise (**c**) during the last deglaciation and Holocene[32]. The AMOC reconstructions are based on $^{231}Pa/^{230}Th$ ratio[40,42] (green) and cross strait $\delta^{18}O$ at the Florida Straits[41] (blue). The gray shading highlights the period of the HMAP with muted AMOC response to FW forcing associated with the ~50-m sea-level rise from the final deglaciation of Northern Hemisphere ice sheets. ka, thousand years before 1950.*

Fig. 2. Comparison of data and models for regional temperature stacks of past 21,000 years. a, *AMOC reconstruction from $^{231}Pa/^{230}Th$ ratio in Bermuda rise[40,42] and modeled maximum AMOC transport (below 500 m in the Atlantic Ocean). Sv, Sverdrup (10^6 m^3 s^{-1}).* ***b-d****, surface air temperature stacks over Greenland (**b**), Antarctica (**d**) and SST stack in the Eastern Atlantic Ocean/Mediterranean Sea (**c**). Proxy data in black; before and include the onset of the Bølling, TraCE-21K-I and TraCE-21K-II are identical (red); after the onset of the Bølling, simulation based on the protocol of prescribing the reconstructed AMOC in red (TraCE-21K-II) and prescribing the reconstructed FW forcing in cyan (TraCE-21K-I). All modeled changes are referenced to the proxy data during the Oldest Dryas (19-15 ka) to aid the comparison. Note that scaling of modeled AMOC versus the $^{231}Pa/^{230}Th$ ratio is only intended to capture the relative range of variability. LGM, last glacial maximum. OD, Oldest Dryas. BA, Bølling-Allerød interstadial. YD, Younger Dryas. HMAP, Holocene Meltwater-AMOC paradox. LH, late Holocene. ka, thousand years before 1950.*

Fig. 3. Differences of modeled surface temperature and precipitation during the early Holocene (9 ka – 6 ka) between simulations with and without FW forcing in the Holocene. *The pattern of the temperature (ºC) and precipitation (mm/year) differences resembles the classic bipolar seesaw pattern with cooling over Greenland and the Eastern Atlantic Ocean/Mediterranean Sea, warming over Antarctica and southward movement of the Intertropical Convergence Zone (ITCZ) due to the reduction of the northward heat transports with the weaker AMOC in TraCE-21K-I[18,48].*

References:

1 Broecker, W. S., Peteet, D. M. & Rind, D. Does the Ocean-Atmosphere System Have More Than One Stable Mode of Operation. *Nature* **315**, 21-26 (1985).

2 Rahmstorf, S. Bifurcations of the Atlantic Thermohaline Circulation in Response to Changes in the Hydrological Cycle. *Nature* **378**, 145-149 (1995).

3 Clark, P. U. *et al.* Freshwater forcing of abrupt climate change during the last glaciation. *Science* **293**, 283-287 (2001).

4 Shakun, J. D. *et al.* Global warming preceded by increasing carbon dioxide concentrations during the last deglaciation. *Nature* **484**, 49-54 (2012).

5 He, F. *et al.* Northern Hemisphere forcing of Southern Hemisphere climate during the last deglaciation. *Nature* **494**, 81-85 (2013).

6 Lenton, T. M. *et al.* Climate tipping points - too risky to bet against. *Nature* **575**, 592-595 (2019).

7 Jackson, L. C. *et al.* Global and European climate impacts of a slowdown of the AMOC in a high resolution GCM. *Climate Dynamics* **45**, 3299-3316 (2015).

8 Yin, J., Schlesinger, M. E. & Stouffer, R. J. Model projections of rapid sea-level rise on the northeast coast of the United States. *Nature Geoscience* **2**, 262-266 (2009).

9 Ritchie, P. D. L. *et al.* Shifts in national land use and food production in Great Britain after a climate tipping point. *Nature Food* **1**, 76-83 (2020).

10 Caesar, L., Rahmstorf, S., Robinson, A., Feulner, G. & Saba, V. Observed fingerprint of a weakening Atlantic Ocean overturning circulation. *Nature* **556**, 191-196 (2018).

11 Fu, Y., Li, F. L., Karstensen, J. & Wang, C. Z. A stable Atlantic Meridional Overturning Circulation in a changing North Atlantic Ocean since the 1990s. *Science Advances* **6**, eabc7836 (2020).

12 Moat, B. *et al.* Pending recovery in the strength of the meridional overturning circulation at 26 degrees N. *Ocean Science* **16**, 863-874 (2020).

13 Bakker, P. *et al.* Fate of the Atlantic Meridional Overturning Circulation: Strong decline under continued warming and Greenland melting. *Geophysical Research Letters* **43**, 12252-12260 (2016).

14 Weijer, W., Cheng, W., Garuba, O. A., Hu, A. & Nadiga, B. T. CMIP6 Models Predict Significant 21st Century Decline of the Atlantic Meridional Overturning Circulation. *Geophysical Research Letters* **47**, e2019GL086075 (2020).

15 Gregory, J. M. *et al.* A model intercomparison of changes in the Atlantic thermohaline circulation in response to increasing atmospheric CO2concentration. *Geophysical Research Letters* **32**, n/a-n/a (2005).

16 Jahn, A. & Holland, M. M. Implications of Arctic sea ice changes for North Atlantic deep convection and the meridional overturning circulation in CCSM4-CMIP5 simulations. *Geophysical Research Letters* **40**, 1206-1211 (2013).

17 Golledge, N. R. *et al.* Global environmental consequences of twenty-first-century ice-sheet melt. *Nature* **566**, 65-72 (2019).

18 Stouffer, R. J. *et al.* Investigating the causes of the response of the thermohaline circulation to past and future climate changes. *Journal of Climate* **19**, 1365-1387 (2006).

19 Weijer, W. *et al.* Stability of the Atlantic Meridional Overturning Circulation: A Review and Synthesis. *Journal of Geophysical Research-Oceans* **124**, 5336-5375 (2019).

20 Rahmstorf, S. On the freshwater forcing and transport of the Atlantic thermohaline circulation. *Climate Dynamics* **12**, 799-811 (1996).

21 Liu, W., Xie, S. P., Liu, Z. & Zhu, J. Overlooked possibility of a collapsed Atlantic Meridional Overturning Circulation in warming climate. *Sci Adv* **3**, e1601666 (2017).

22 Gnanadesikan, A., Kelson, R. & Sten, M. Flux Correction and Overturning Stability: Insights from a Dynamical Box Model. *Journal of Climate* **31**, 9335-9350 (2018).

23 Wunsch, C. Towards understanding the Paleocean. *Quaternary Science Reviews* **29**, 1960-1967 (2010).

24 Condron, A. & Winsor, P. Meltwater routing and the Younger Dryas. *Proc Natl Acad Sci U S A* **109**, 19928-19933 (2012).

25 Kim, H.-J., An, S.-I., Kim, S.-K. & Park, J.-H. Feedback Processes Modulating the Sensitivity of Atlantic Thermohaline Circulation to Freshwater Forcing Timescales. *Journal of Climate* **34**, 5081-5092 (2021).

26 Jackson, L. C. & Wood, R. A. Hysteresis and Resilience of the AMOC in an Eddy-Permitting GCM. *Geophysical Research Letters* **45**, 8547-8556 (2018).

27 Lozier, M. S. *et al.* A sea change in our view of overturning in the subpolar North Atlantic. *Science* **363**, 516-521 (2019).

28 Swingedouw, D. *et al.* Decadal fingerprints of freshwater discharge around Greenland in a multi-model ensemble. *Climate Dynamics* **41**, 695-720 (2012).

29 Jackson, L. C. *et al.* Impact of ocean resolution and mean state on the rate of AMOC weakening. *Climate Dynamics* **55**, 1711-1732 (2020).

30 Ullman, D. J. *et al.* Final Laurentide ice-sheet deglaciation and Holocene climate-sea level change. *Quaternary Science Reviews* **152**, 49-59 (2016).

31 Cuzzone, J. K. *et al.* Final deglaciation of the Scandinavian Ice Sheet and implications for the Holocene global sea-level budget. *Earth and Planetary Science Letters* **448**, 34-41 (2016).

32 Lambeck, K., Rouby, H., Purcell, A., Sun, Y. & Sambridge, M. Sea level and global ice volumes from the Last Glacial Maximum to the Holocene. *Proc Natl Acad Sci U S A* **111**, 15296-15303 (2014).

33 Licciardi, J. M., Clark, P. U., Jenson, J. W. & Macayeal, D. R. Deglaciation of a soft-bedded Laurentide Ice Sheet. *Quaternary Science Reviews* **17**, 427-448 (1998).

34 Licciardi, J. M., Teller, J. T. & Clark, P. U. in *Mechanisms of Global Climate Change at Millennial Time Scales* Vol. 112 *Geophysical Monograph Series* 177-201 (AGU, 1999).

35 Carlson, A. E. *et al.* Rapid early Holocene deglaciation of the Laurentide ice sheet. *Nature Geoscience* **1**, 620-624 (2008).

36 Siegert, M. J. & Dowdeswell, J. A. Numerical reconstructions of the Eurasian Ice Sheet and climate during the Late Weichselian. *Quaternary Science Reviews* **23**, 1273-1283 (2004).

37 Dixon, K. W., Delworth, T. L., Spelman, M. J. & Stouffer, R. J. The influence of transient surface fluxes on North Atlantic overturning in a coupled GCM climate change experiment. *Geophysical Research Letters* **26**, 2749-2752 (1999).

38 Haine, T. W. N. *et al.* Arctic freshwater export: Status, mechanisms, and prospects. *Global and Planetary Change* **125**, 13-35 (2015).

39 Clark, J., Mitrovica, J. X. & Alder, J. Coastal paleogeography of the California–Oregon–Washington and Bering Sea continental shelves during the latest Pleistocene and

Holocene: implications for the archaeological record. *Journal of Archaeological Science* **52**, 12-23 (2014).

40 Lippold, J. *et al.* Constraining the Variability of the Atlantic Meridional Overturning Circulation During the Holocene. *Geophysical Research Letters* **46**, 11338-11346 (2019).

41 Lynch-Stieglitz, J. The Atlantic Meridional Overturning Circulation and Abrupt Climate Change. *Ann Rev Mar Sci* **9**, 83-104 (2017).

42 McManus, J. F., Francois, R., Gherardi, J. M., Keigwin, L. D. & Brown-Leger, S. Collapse and rapid resumption of Atlantic meridional circulation linked to deglacial climate changes. *Nature* **428**, 834-837 (2004).

43 Ng, H. C. *et al.* Coherent deglacial changes in western Atlantic Ocean circulation. *Nat Commun* **9**, 2947 (2018).

44 Alley, R. B. *et al.* Holocene climatic instability: A prominent, widespread event 8200 yr ago. *Geology* **25**, 483-486 (1997).

45 Fleitmann, D. *et al.* Evidence for a widespread climatic anomaly at around 9.2 ka before present. *Paleoceanography* **23**, n/a-n/a (2008).

46 Bond, G. *et al.* A pervasive millennial-scale cycle in North Atlantic Holocene and glacial climates. *Science* **278**, 1257-1266 (1997).

47 Buizert, C. *et al.* Greenland temperature response to climate forcing during the last deglaciation. *Science* **345**, 1177-1180 (2014).

48 Liu, Z. *et al.* Transient simulation of last deglaciation with a new mechanism for Bolling-Allerod warming. *Science* **325**, 310-314 (2009).

49 He, F. *Simulating transient climate evolution of the last deglaciation with CCSM3* Ph.D. thesis, The University of Wisconsin - Madison, (2011).

50 Zhang, Y., Renssen, H., Seppä, H. & Valdes, P. J. Holocene temperature trends in the extratropical Northern Hemisphere based on inter-model comparisons. *Journal of Quaternary Science* **33**, 464-476 (2018).

51 Renssen, H. *et al.* The spatial and temporal complexity of the Holocene thermal maximum. *Nature Geoscience* **2**, 411-414 (2009).

52 Renold, M., Raible, C. C., Yoshimori, M. & Stocker, T. F. Simulated resumption of the North Atlantic meridional overturning circulation – Slow basin-wide advection and abrupt local convection. *Quaternary Science Reviews* **29**, 101-112 (2010).

53 Zhu, J., Liu, Z. Y., Zhang, X., Eisenman, I. & Liu, W. Linear weakening of the AMOC in response to receding glacial ice sheets in CCSM3. *Geophysical Research Letters* **41**, 6252-6258 (2014).

54 Du, J., Haley, B. A. & Mix, A. C. Evolution of the Global Overturning Circulation since the Last Glacial Maximum based on marine authigenic neodymium isotopes. *Quaternary Science Reviews* **241**, 106396 (2020).

55 Missiaen, L. *et al.* Modelling the impact of biogenic particle flux intensity and composition on sedimentary Pa/Th. *Quaternary Science Reviews* **240**, 106394 (2020).

56 Bova, S., Rosenthal, Y., Liu, Z., Godad, S. P. & Yan, M. Seasonal origin of the thermal maxima at the Holocene and the last interglacial. *Nature* **589**, 548-553 (2021).

57 Kaufman, D. S. *et al.* Holocene thermal maximum in the western Arctic (0–180°W). *Quaternary Science Reviews* **23**, 529-560 (2004).

58 Marcott, S. A., Shakun, J. D., Clark, P. U. & Mix, A. C. A reconstruction of regional and global temperature for the past 11,300 years. *Science* **339**, 1198-1201 (2013).

59 Liu, Z. *et al.* The Holocene temperature conundrum. *Proc Natl Acad Sci U S A* **111**, E3501-3505 (2014).

60 Park, H.-S., Kim, S.-J., Stewart, A. L., Son, S.-W. & Seo, K.-H. Mid-Holocene Northern Hemisphere warming driven by Arctic amplification. *Science Advances* **5**, eaax8203 (2019).

61 He, F. *et al.* Simulating global and local surface temperature changes due to Holocene anthropogenic land cover change. *Geophysical Research Letters* **41**, 623-631 (2014).

62 Carlson, A. E. & Clark, P. U. Ice sheet sources of sea level rise and freshwater discharge during the last deglaciation. *Reviews of Geophysics* **50**, RG4007 (2012).

63 Broecker, W. S. Geology. Was the Younger Dryas triggered by a flood? *Science* **312**, 1146-1148 (2006).

64 Rahmstorf, S. Ocean circulation and climate during the past 120,000 years. *Nature* **419**, 207-214 (2002).

65 Sigman, D. M., Hain, M. P. & Haug, G. H. The polar ocean and glacial cycles in atmospheric CO(2) concentration. *Nature* **466**, 47-55 (2010).

66 Collins, M. *et al. Long-term climate change: projections, commitments and irreversibility. In: Climate Change 2013: The Physical Science Basis. Contribution of Working Group I to the Fifth Assessment Report of the Intergovernmental Panel on Climate Change [Stocker, T.F., D. Qin, G.-K. Plattner, M. Tignor, S.K. Allen, J. Boschung, A. Nauels, Y. Xia, V. Bex and P.M. Midgley (eds.)]*. (2013).

67 Church, J. A. *et al. Sea Level Change. In: Climate Change 2013: The Physical Science Basis. Contribution of Working Group I to the Fifth Assessment Report of the Intergovernmental Panel on Climate Change [Stocker, T.F., D. Qin, G.-K. Plattner, M. Tignor, S.K. Allen, J. Boschung, A. Nauels, Y. Xia, V. Bex and P.M. Midgley (eds.)]*. (Cambridge University Press, 2013).

68 Briner, J. P. *et al.* Rate of mass loss from the Greenland Ice Sheet will exceed Holocene values this century. *Nature* **586**, 70-+ (2020).

69 Aschwanden, A. *et al.* Contribution of the Greenland Ice Sheet to sea level over the next millennium. *Sci Adv* **5**, eaav9396 (2019).

70 Alley, R. B. The Younger Dryas cold interval as viewed from central Greenland. *Quaternary Science Reviews* **19**, 213-226 (2000).

Methods

Transient climate modelling

We conducted version II of the TraCE-21K simulation (TraCE-21K-II) at the Computational and Information Systems Laboratory[71,72] of National Center for Atmospheric Research with the Community Climate System Model version 3 (CCSM3) based on the protocol of prescribing the reconstructed AMOC instead of the reconstructed FW forcing, which removes the temperature and precipitation biases in the Holocene segment of the first transient simulation of past 21,000 years (TraCE-21K-I)[48,49] due to the overestimation of the response of AMOC to freshwater fluxes in the coupled global climate models. TraCE-21K-II was conducted with the same climatic forcing from Earth's orbital variations and greenhouse gases as well as similar ice sheets variations as in TraCE-21K-I[49], but with no freshwater flux being prescribed when the reconstructed AMOC exhibits typical interglacial strength during the Bølling-Allerød interstadial (~14.7 ka – 12.9 ka) and throughout the Holocene from ~11,500 years ago to present day.

Between the LGM and the onset of the Bølling (~14.7 ka), TraCE-21K-I and TraCE-21K-II are identical. TraCE-21K-II was first branched off from the 14.9 ka (ka, thousand years before 1950) of TraCE-21K-I with meltwater fluxes being totally cut off at the onset of Bølling warming around 14.7 ka. Between Bølling warming and the Younger Dryas, no meltwater flux was applied in TraCE-21K-II, which has been demonstrated to be able to produce a reasonable simulation of both Bølling interstadial over Greenland and the Antarctic Cold Reversal over Antarctica and the Southern Ocean[73]. During the Younger Dryas, a meltwater flux of 0.17 Sv was applied in the North Atlantic Ocean (50ºN-70ºN) between 12.9 ka and 11.7 ka in TraCE-21K-II to slow the AMOC down to the minimum of ~4 Sv in CCSM3 (Extended Data Figs. 6-7 and Supplementary Table 3) and produce reasonable simulation of cooling over the Greenland and Eastern Atlantic/Mediterranean region[47] (Fig. 2). At the end of the Younger Dryas, the meltwater forcing was ceased at 11.7 ka and no further meltwater was applied in TraCE-21K-II throughout the Holocene. As a result, the AMOC in TraCE-21K-II during the HMAP is much stronger than that in TraCE-21K-I due to stronger deep water formation associated with deeper winter mix layer depth in TraCE-21K-II (Extended Data Fig. 10). Note that for the Holocene segment of the TraCE-21K-I experiment, contributions to the FW forcing include the sustained ~0.1 Sv meltwater flux from Northern Hemisphere ice sheets and inflow of fresher North Pacific water to the North Atlantic associated with the opening of Bering Strait. After 6 ka, the ~0.1 Sv meltwater flux from Northern Hemisphere ice sheets ended, but the inflow of fresher North Pacific water to the North Atlantic associated with the opening of Bering Strait continued. In order to conduct TraCE-21K-II with no freshwater flux throughout the Holocene, the Bering Strait was kept closed to prevent the inflow of fresher North Pacific water to the North Atlantic, which thus explains the difference between TraCE-21K-II and TraCE-21K-I after 6 ka. As in TraCE-21K-I, TraCE-21K-II includes dynamic vegetation feedback and a fixed annual cycle of aerosol forcing[49].

Regional temperature stacks

The ice-core and Eastern Atlantic/Mediterranean regional temperature stacks were derived from the deglacial proxy record compilations[4,47] that contain most published high-resolution (median resolution = 200 years), well-dated (636 radiocarbon dates) temperature records from the last deglaciation, and as such, represent the current state of knowledge on deglacial temperature variability in those regions. The data were linearly interpolated to 100-year resolution and combined as averages to yield mean temperature time series for the regional temperature stacks. The detailed information of all proxy data for regional temperature stacks is documented in Supplementary Table 1 with the locations plotted in Extended Data Fig. 1. All modeled regional temperature stacks are derived as averages of simulated annual mean temperature with 10-year averages at proxy site locations. Figure 2 shows the comparison between the model and data for regional temperature stacks of past 21,000 years with changes in modeled regional temperature stacks referenced to the averages of proxy regional temperature stacks during the Oldest Dryas (19-15 ka). Extended Data Fig. 4 shows the comparison of regional temperature stacks between data and models with temperature anomalies of each regional stack from the average value in the Oldest Dryas (19 ka-15 ka).

Data Availability

The model datasets used for this study (Figs. 2-3) are available from the Open Science Framework (https://doi.org/10.17605/OSF.IO/NUQ2K). TraCE-21K-I model data are available from the Earth System Grid https://www.earthsystemgrid.org/project/trace.html and TraCE-21K-II model data are available from the Transient Climate Simulation Lab https://trace-21k.nelson.wisc.edu.

Code Availability

CCSM3 is freely available as open-source code from http://www.cesm.ucar.edu/models/ccsm3.0/

Methods Reference:

71 Computational Information Systems Laboratory. Yellowstone: IBM iDataPlex System (University Community Computing). Boulder, CO: National Center for Atmospheric Research. http://n2t.net/ark:/85065/d7wd3xhc. (2016).

72 Computational Information Systems Laboratory. Cheyenne: HPE/SGI ICE XA System (University Community Computing). Boulder, CO: National Center for Atmospheric Research. doi:10.5065/D6RX99HX. (2019).

73 Pedro, J. B. *et al.* The spatial extent and dynamics of the Antarctic Cold Reversal. *Nature Geoscience* **9**, 51-55 (2015).

74 Rasmussen, S. O. *et al.* A new Greenland ice core chronology for the last glacial termination. *Journal of Geophysical Research* **111** (2006).

75 Andersen, K. K. *et al.* The Greenland Ice Core Chronology 2005, 15–42ka. Part 1: constructing the time scale. *Quaternary Science Reviews* **25**, 3246-3257 (2006).

76 Waelbroeck, C. *et al.* The timing of the last deglaciation in North Atlantic climate records. *Nature* **412**, 724-727 (2001).

77 Cacho, I. *et al.* Variability of the western Mediterranean Sea surface temperature during the last 25,000 years and its connection with the Northern Hemisphere climatic changes. *Paleoceanography* **16**, 40-52 (2001).

78 Bard, E., Rostek, F., Turon, J. L. & Gendreau, S. Hydrological impact of heinrich events in the subtropical northeast atlantic. *Science* **289**, 1321-1324 (2000).

79 Cacho, I. *et al.* Dansgaard-Oeschger and heinrich event imprints in Alboran Sea paleotemperatures. *Paleoceanography* **14**, 698-705 (1999).

80 Castañeda, I. S. *et al.* Millennial-scale sea surface temperature changes in the eastern Mediterranean (Nile River Delta region) over the last 27,000 years. *Paleoceanography* **25** (2010).

81 Arz, H. W., Patzold, J., Muller, P. J. & Moammar, M. O. Influence of Northern Hemisphere climate and global sea level rise on the restricted Red Sea marine environment during termination I. *Paleoceanography* **18** (2003).

82 Stenni, B. *et al.* The deuterium excess records of EPICA Dome C and Dronning Maud Land ice cores (East Antarctica). *Quaternary Science Reviews* **29**, 146-159 (2010).

83 Lemieux-Dudon, B. *et al.* Consistent dating for Antarctic and Greenland ice cores. *Quaternary Science Reviews* **29**, 8-20 (2010).

84 Kawamura, K. *et al.* Northern Hemisphere forcing of climatic cycles in Antarctica over the past 360,000 years. *Nature* **448**, 912-916 (2007).

85 Petit, J. R. *et al.* Climate and atmospheric history of the past 420,000 years from the Vostok ice core, Antarctica. *Nature* **399**, 429-436 (1999).

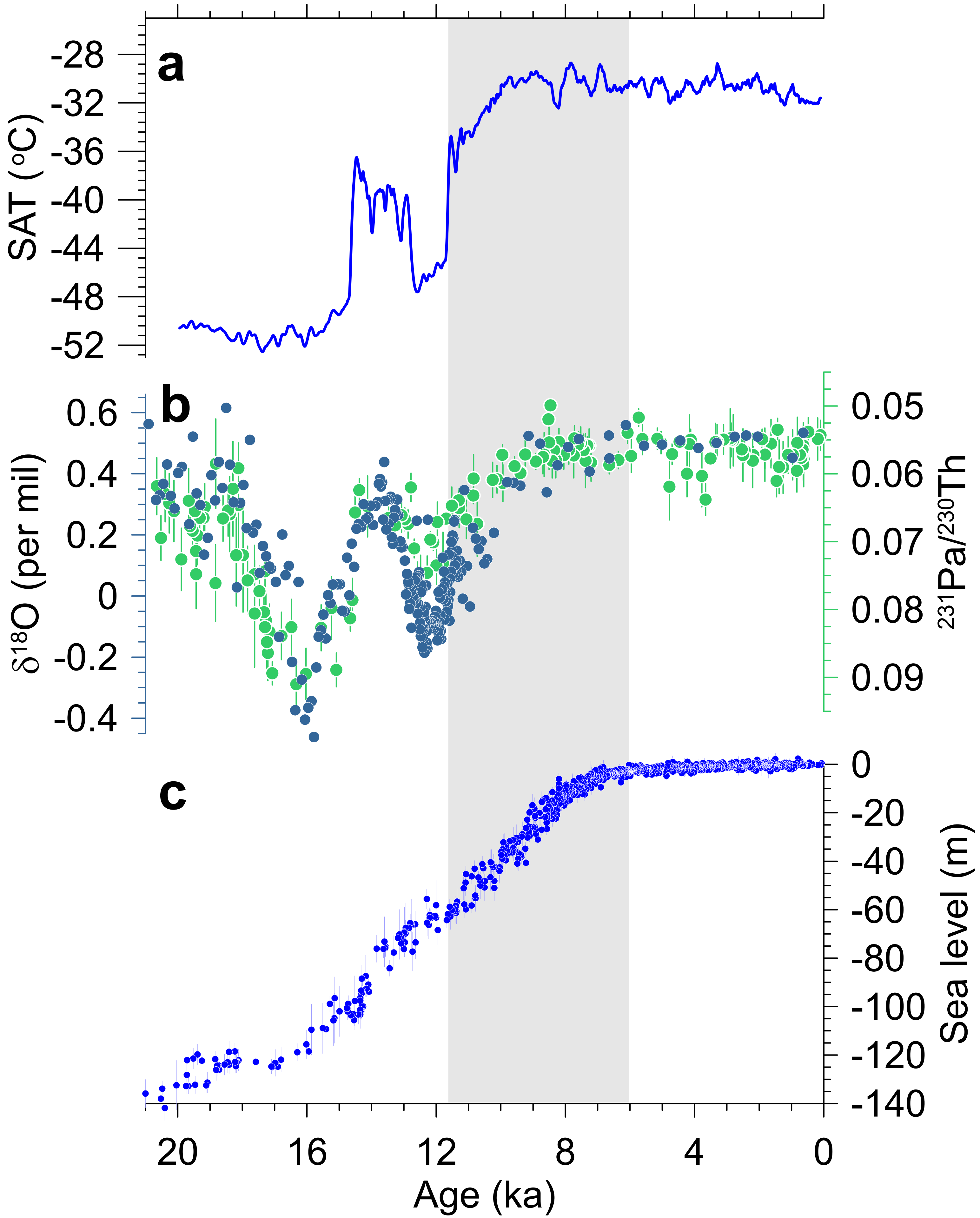
a
SAT (°C)
-28
-32
-36
-40
-44
-48
-52
b
δ18O (per mil)
0.6
0.4
0.2
0
-0.2
-0.4
231Pa/230Th
0.05
0.06
0.07
0.08
0.09
c
Sea level (m)
0
-20
-40
-60
-80
-100
-120
-140
20
16
12
8
4
0
Age (ka)

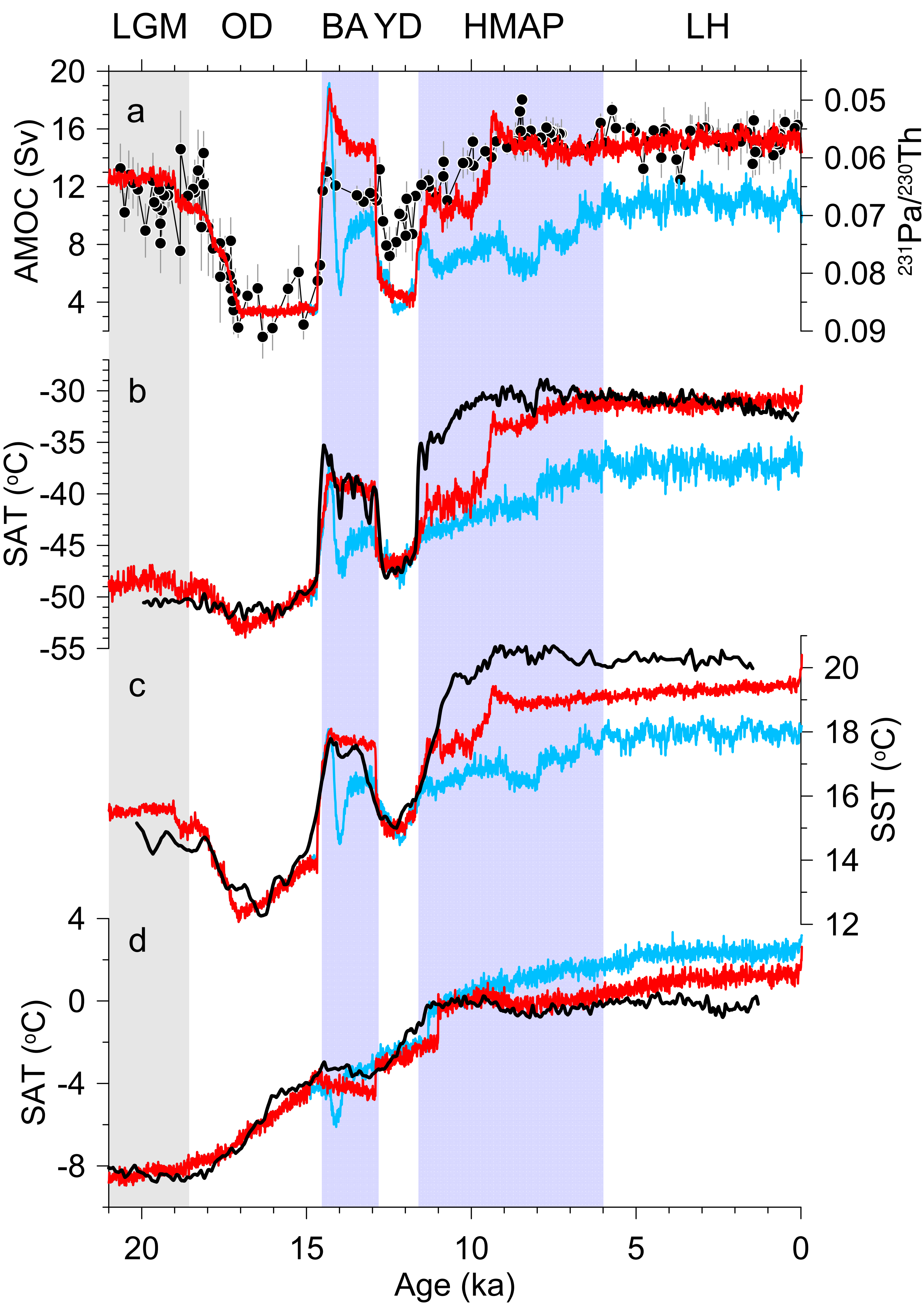

LGM
OD
BA
YD
HMAP
LH
a
b
c
d
AMOC (Sv)
^{231}Pa/^{230}Th
SAT (°C)
SST (°C)
SAT (°C)
Age (ka)
20
16
12
8
4
0.05
0.06
0.07
0.08
0.09
-30
-35
-40
-45
-50
-55
20
18
16
14
12
4
0
-4
-8
20
15
10
5
0

Surface temperature

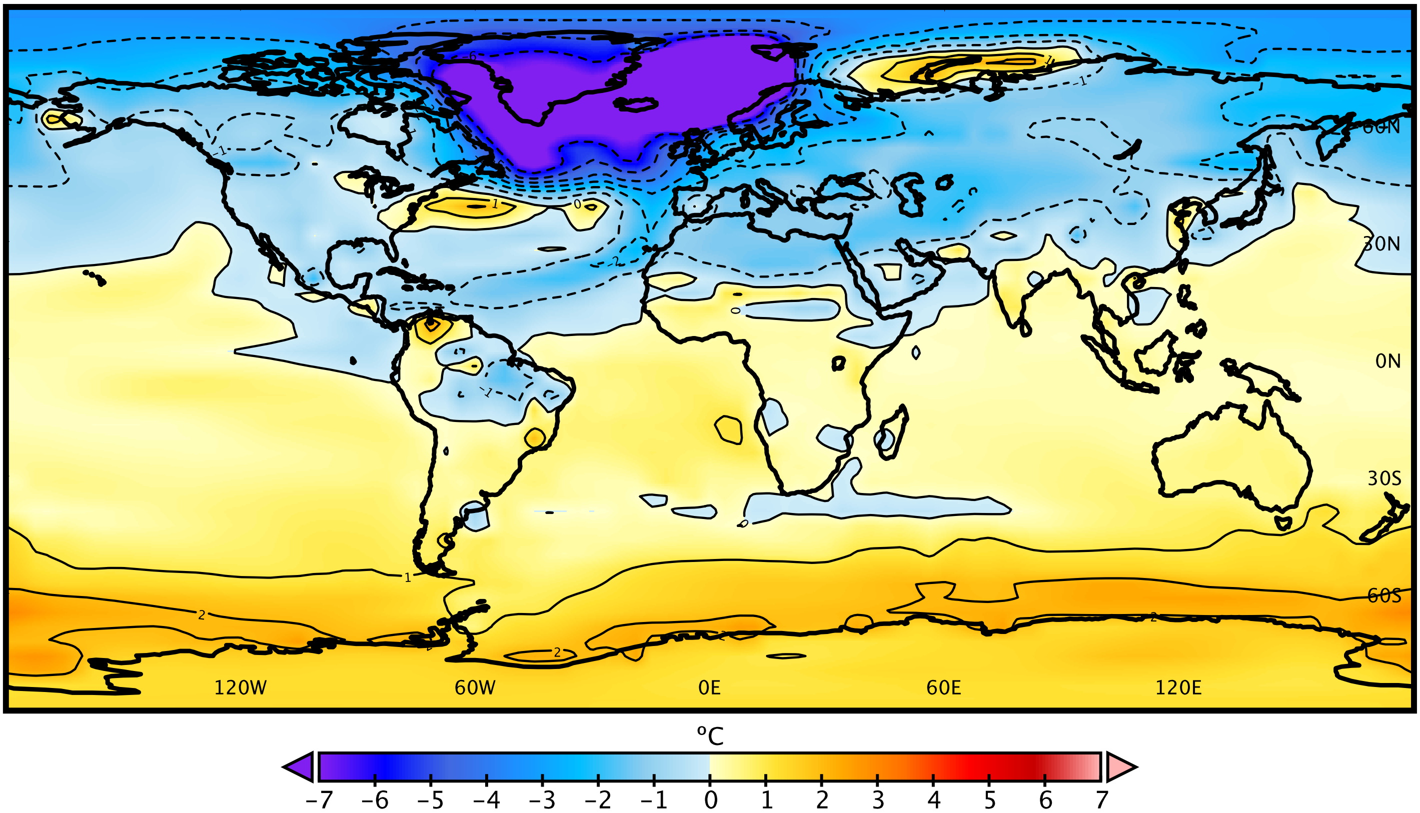

Precipitation rate

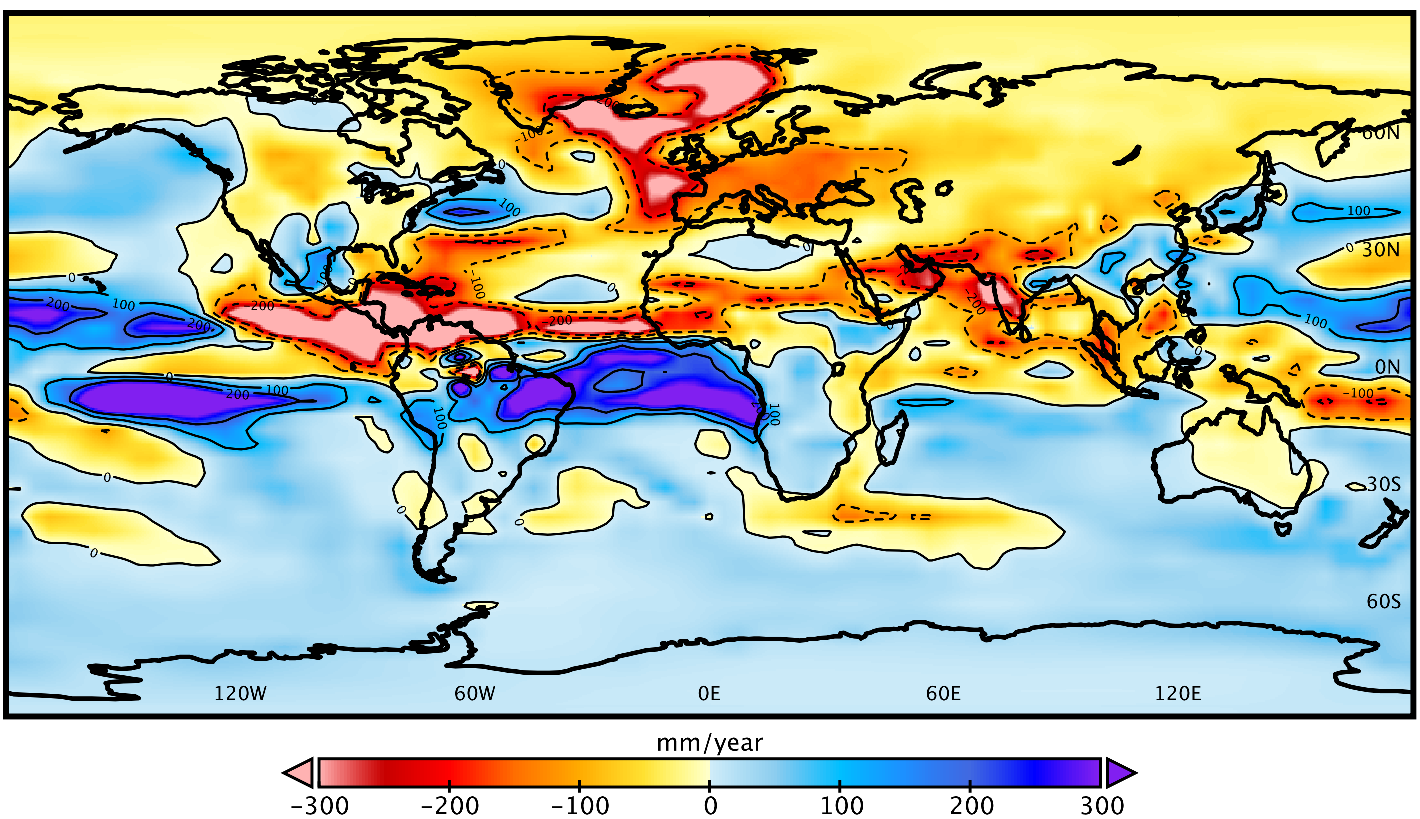

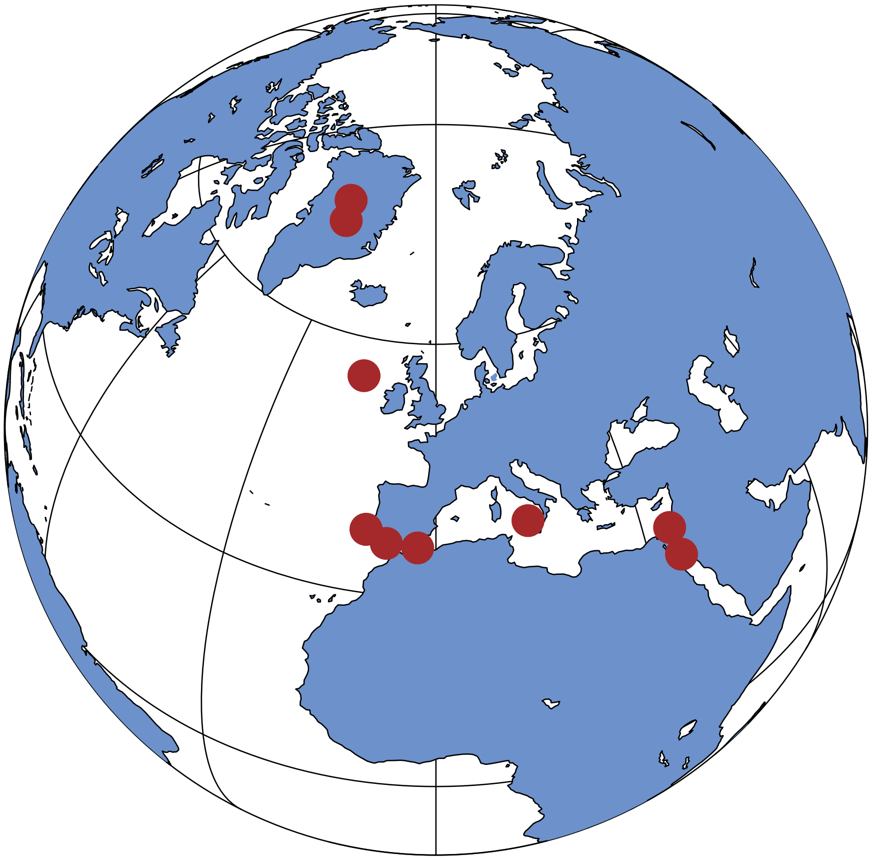

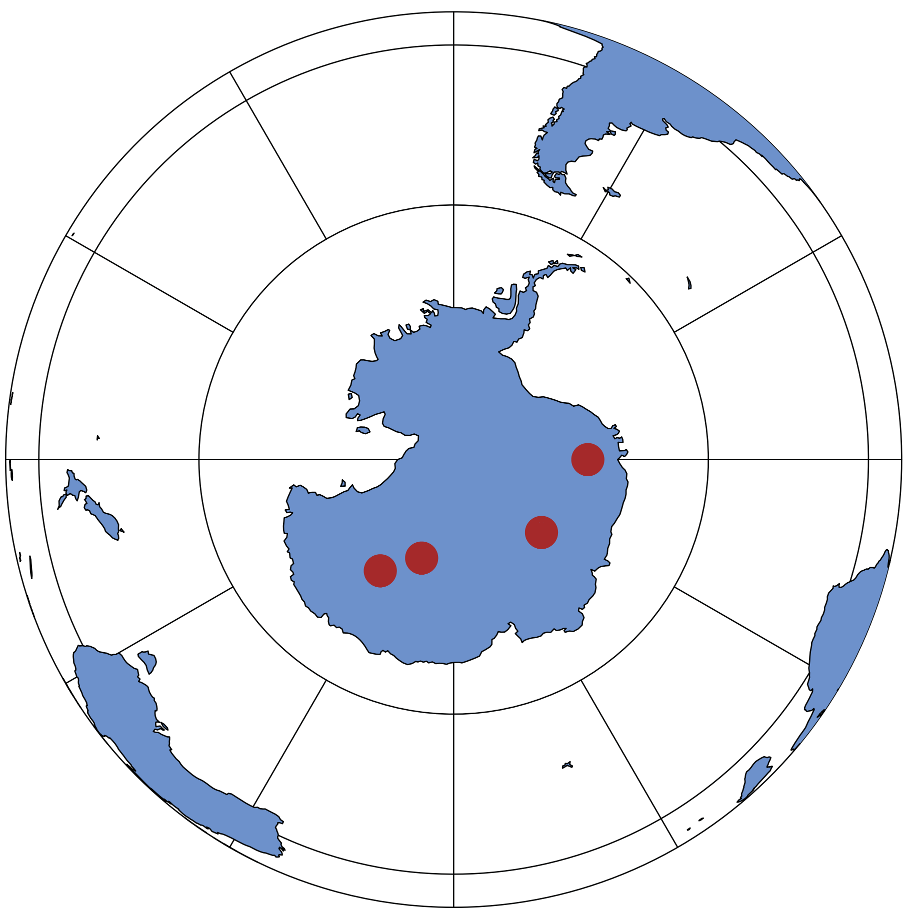

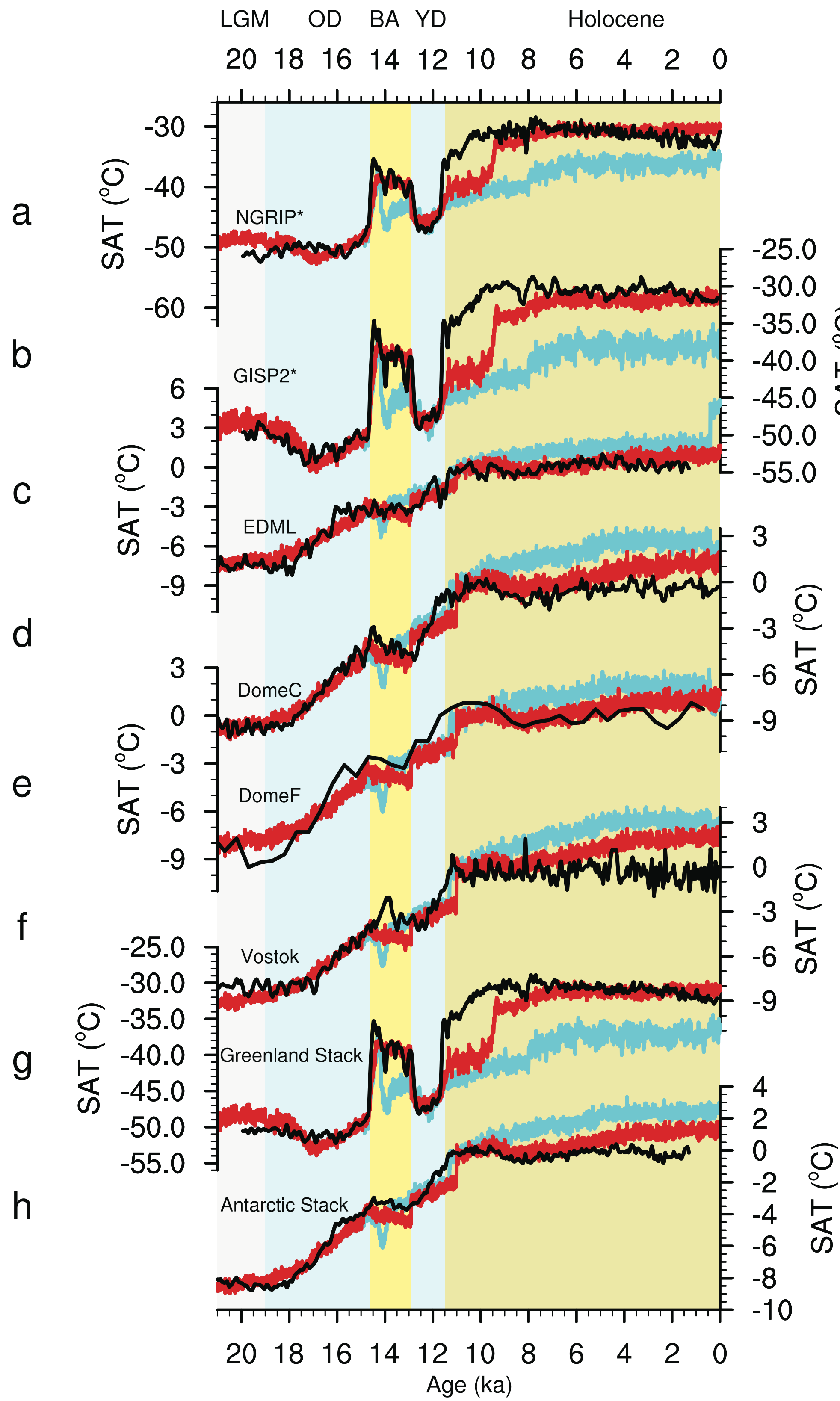

LGM
OD
BA
YD
Holocene
a
b
c
d
e
f
g
h
NGRIP*
GISP2*
EDML
DomeC
DomeF
Vostok
Greenland Stack
Antarctic Stack
SAT (°C)
Age (ka)

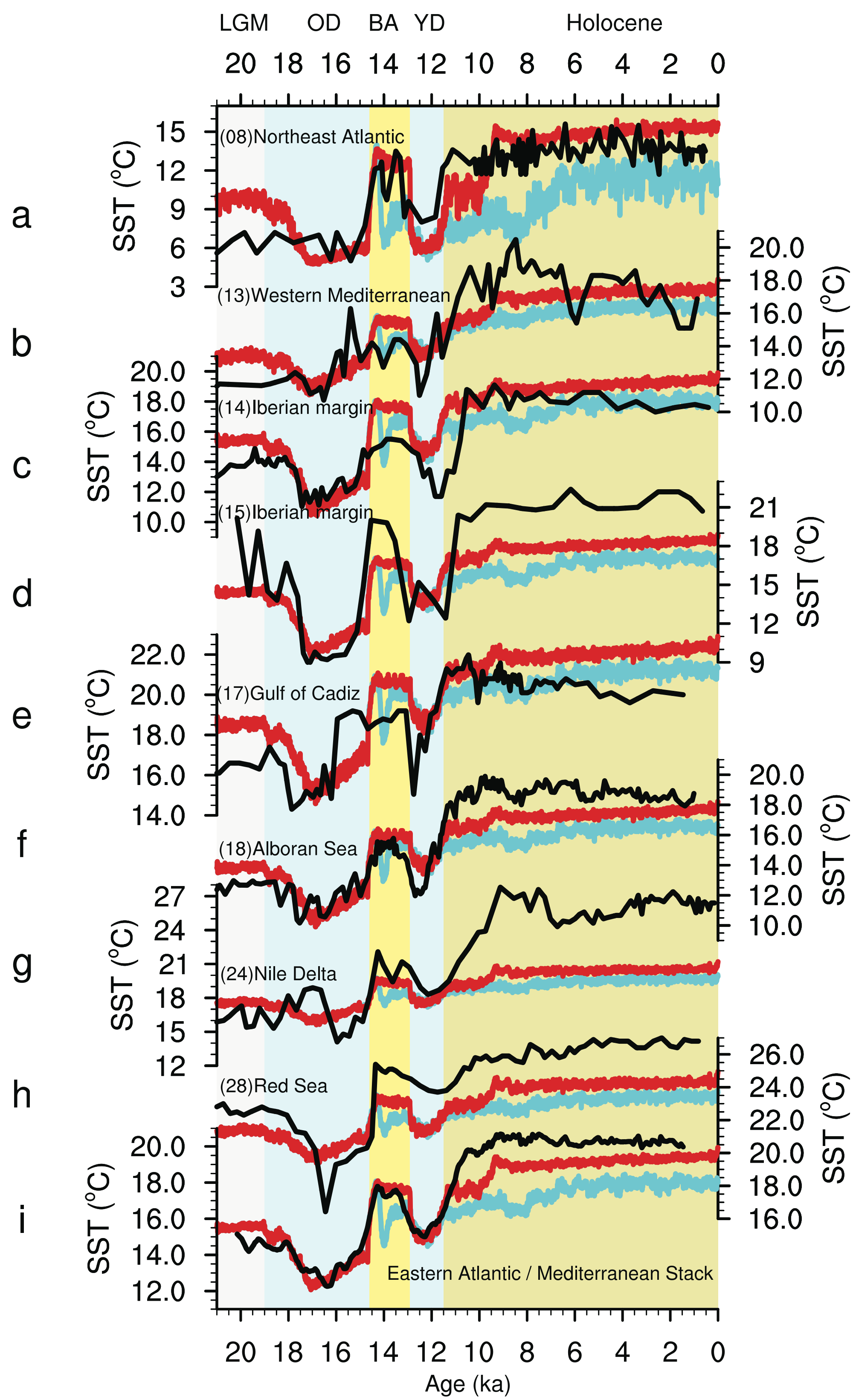

LGM
OD
BA
YD
Holocene
Age (ka)
SST (°C)
a
b
c
d
e
f
g
h
i
(08)Northeast Atlantic
(13)Western Mediterranean
(14)Iberian margin
(15)Iberian margin
(17)Gulf of Cadiz
(18)Alboran Sea
(24)Nile Delta
(28)Red Sea
Eastern Atlantic / Mediterranean Stack

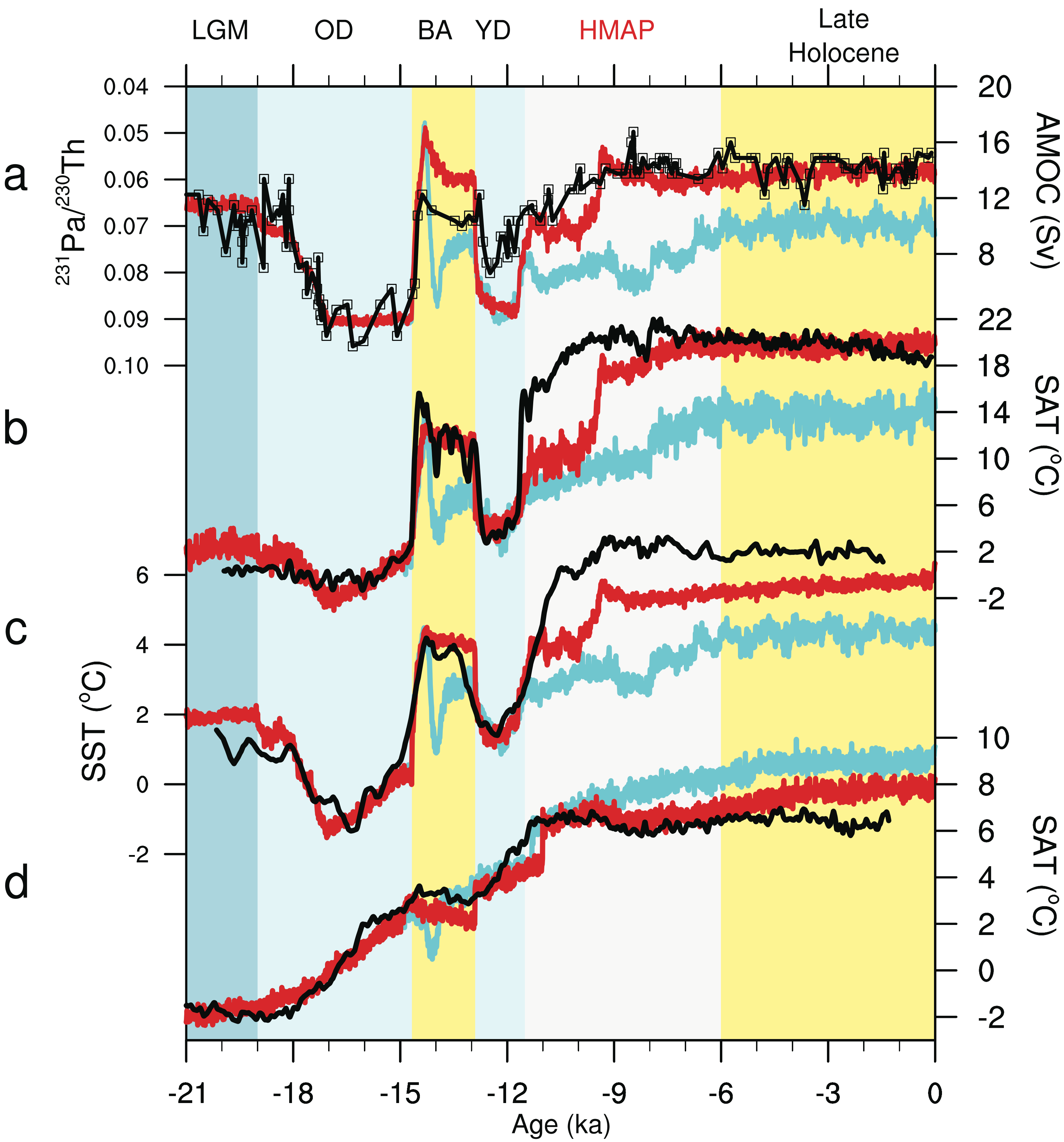

LGM
OD
BA
YD
HMAP
Late Holocene
a
b
c
d
$^{231}Pa/^{230}Th$
0.04
0.05
0.06
0.07
0.08
0.09
0.10
AMOC (Sv)
20
16
12
8
SAT (°C)
22
18
14
10
6
2
-2
SST (°C)
6
4
2
0
-2
SAT (°C)
10
8
6
4
2
0
-2
-21
-18
-15
-12
-9
-6
-3
0
Age (ka)

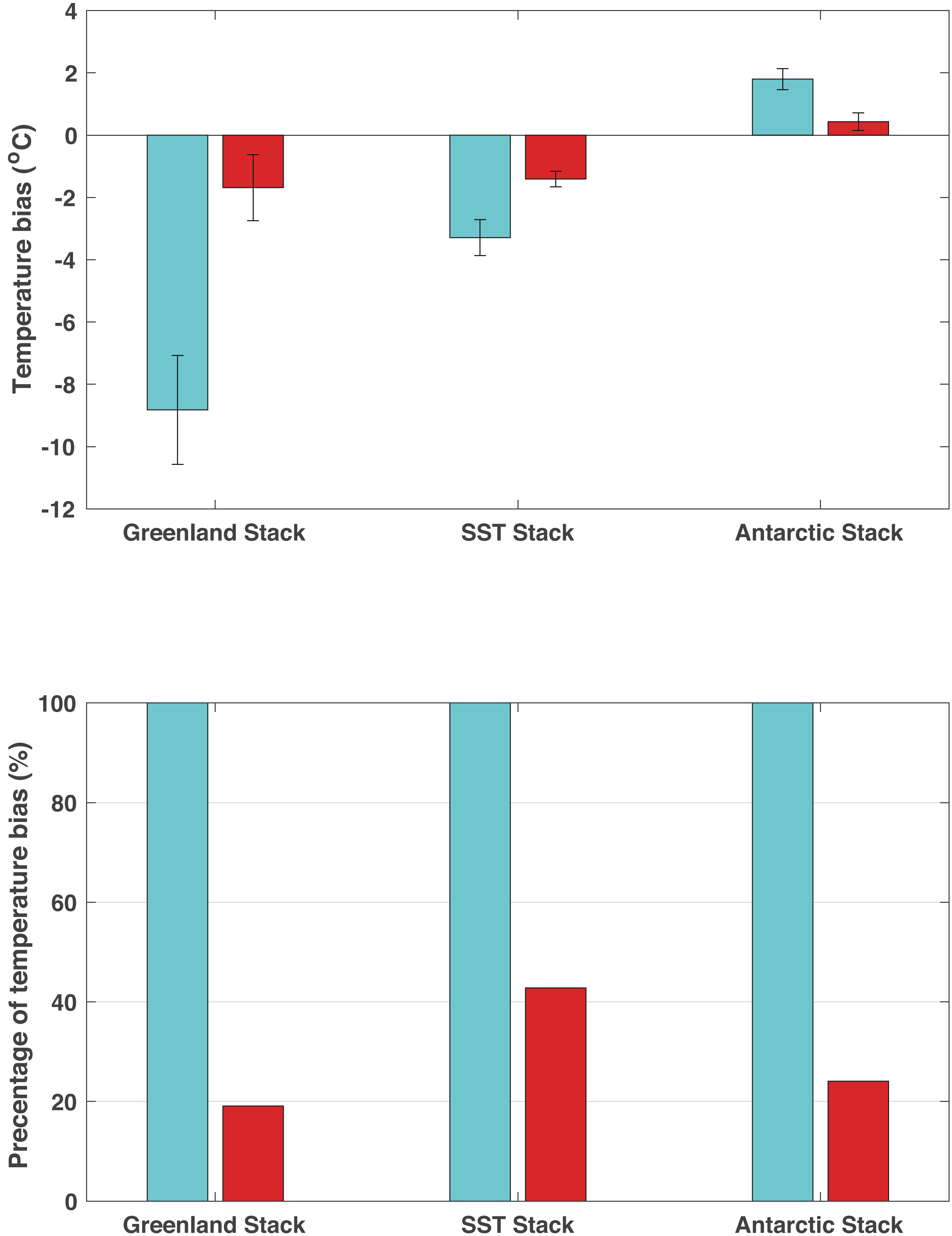

Temperature bias (°C)
4
2
0
-2
-4
-6
-8
-10
-12
Greenland Stack
SST Stack
Antarctic Stack
Precentage of temperature bias (%)
100
80
60
40
20
0
Greenland Stack
SST Stack
Antarctic Stack

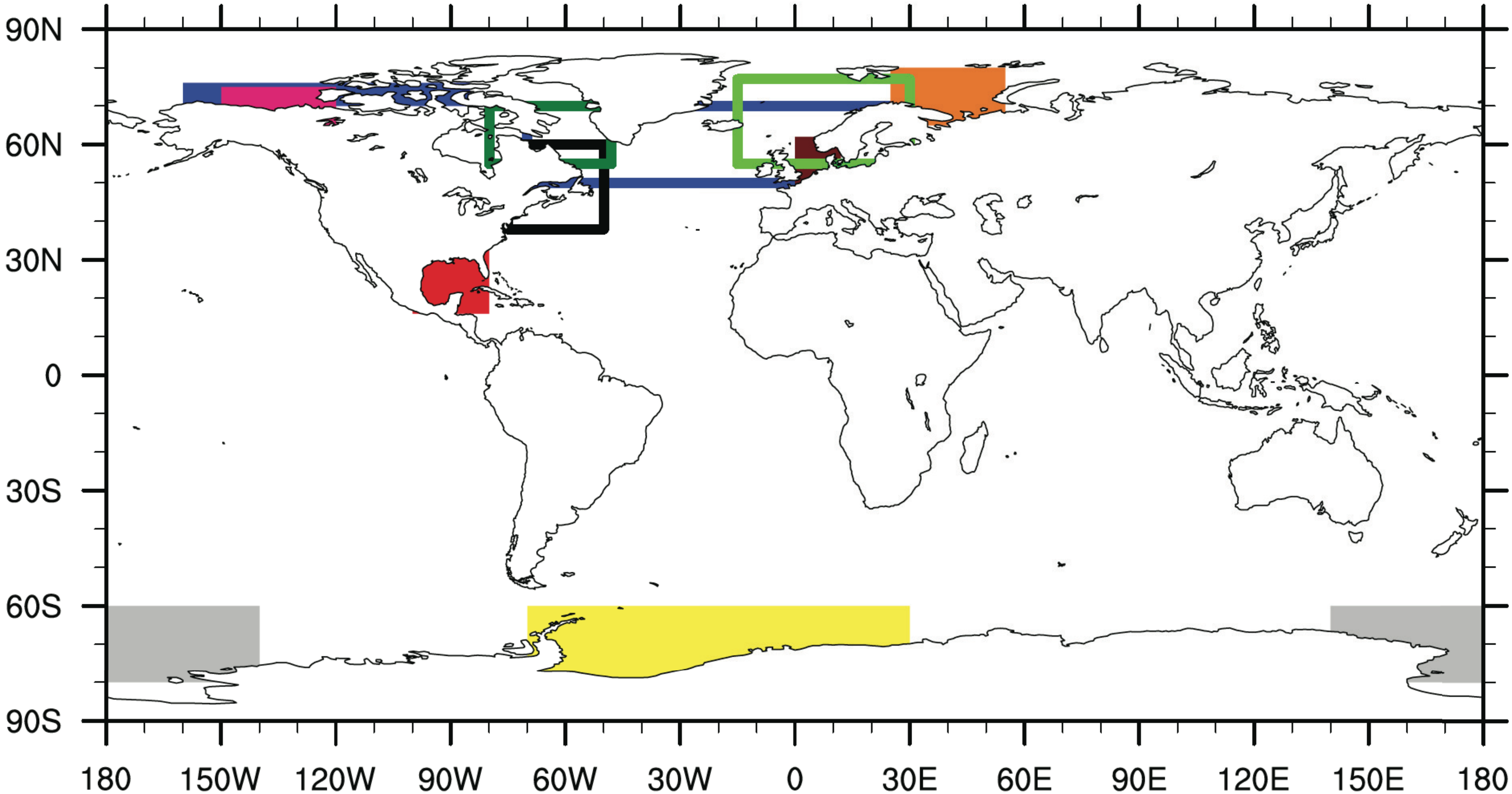
90N
60N
30N
0
30S
60S
90S
180
150W
120W
90W
60W
30W
0
30E
60E
90E
120E
150E
180

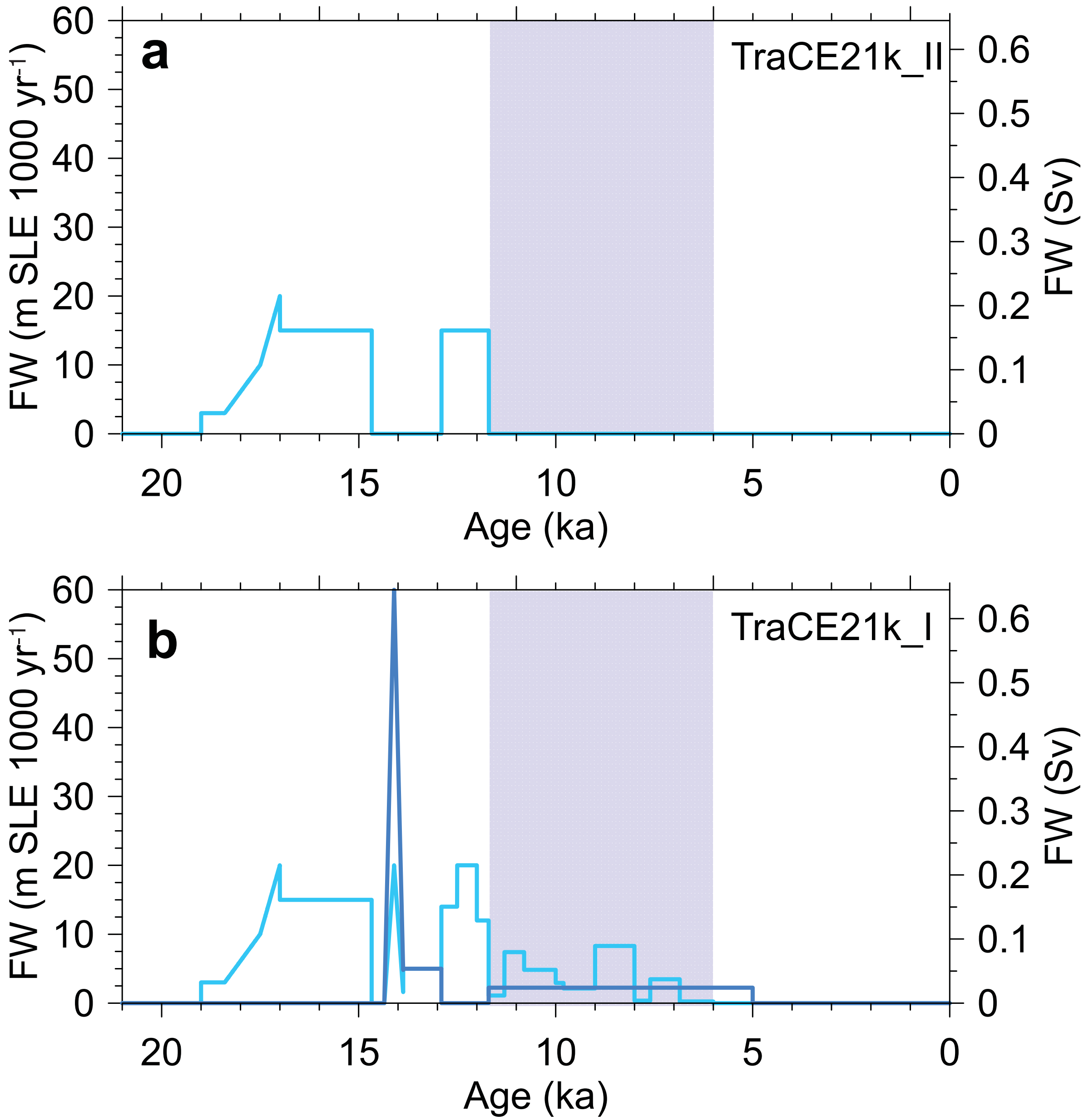
a
TraCE21k_II
b
TraCE21k_I
FW (m SLE 1000 yr⁻¹)
FW (Sv)
Age (ka)
60
50
40
30
20
10
0
0.6
0.5
0.4
0.3
0.2
0.1
20
15
10
5

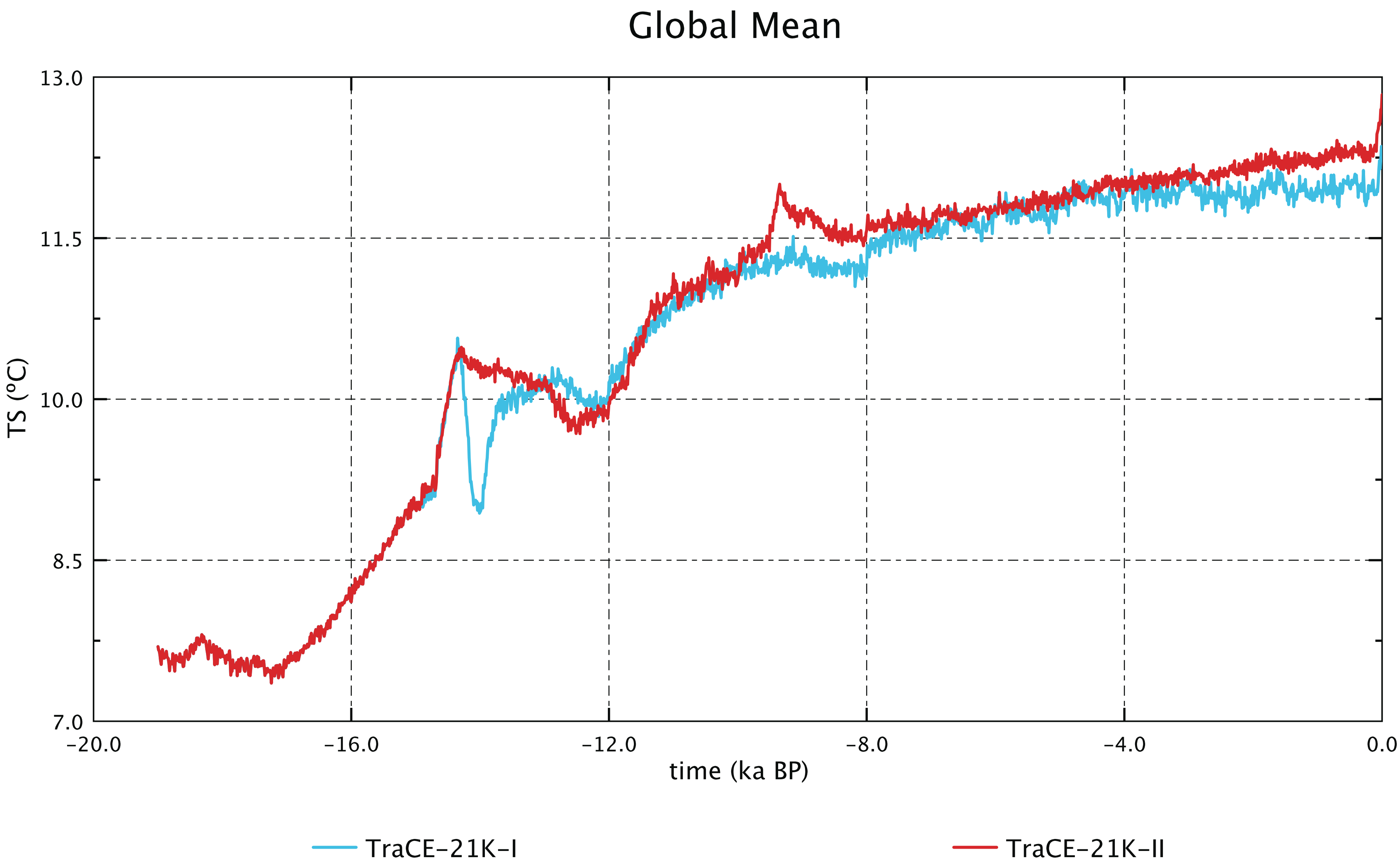
Global Mean
TS (°C)
13.0
11.5
10.0
8.5
7.0
−20.0
−16.0
−12.0
−8.0
−4.0
0.0
time (ka BP)
TraCE−21K−I
TraCE−21K−II

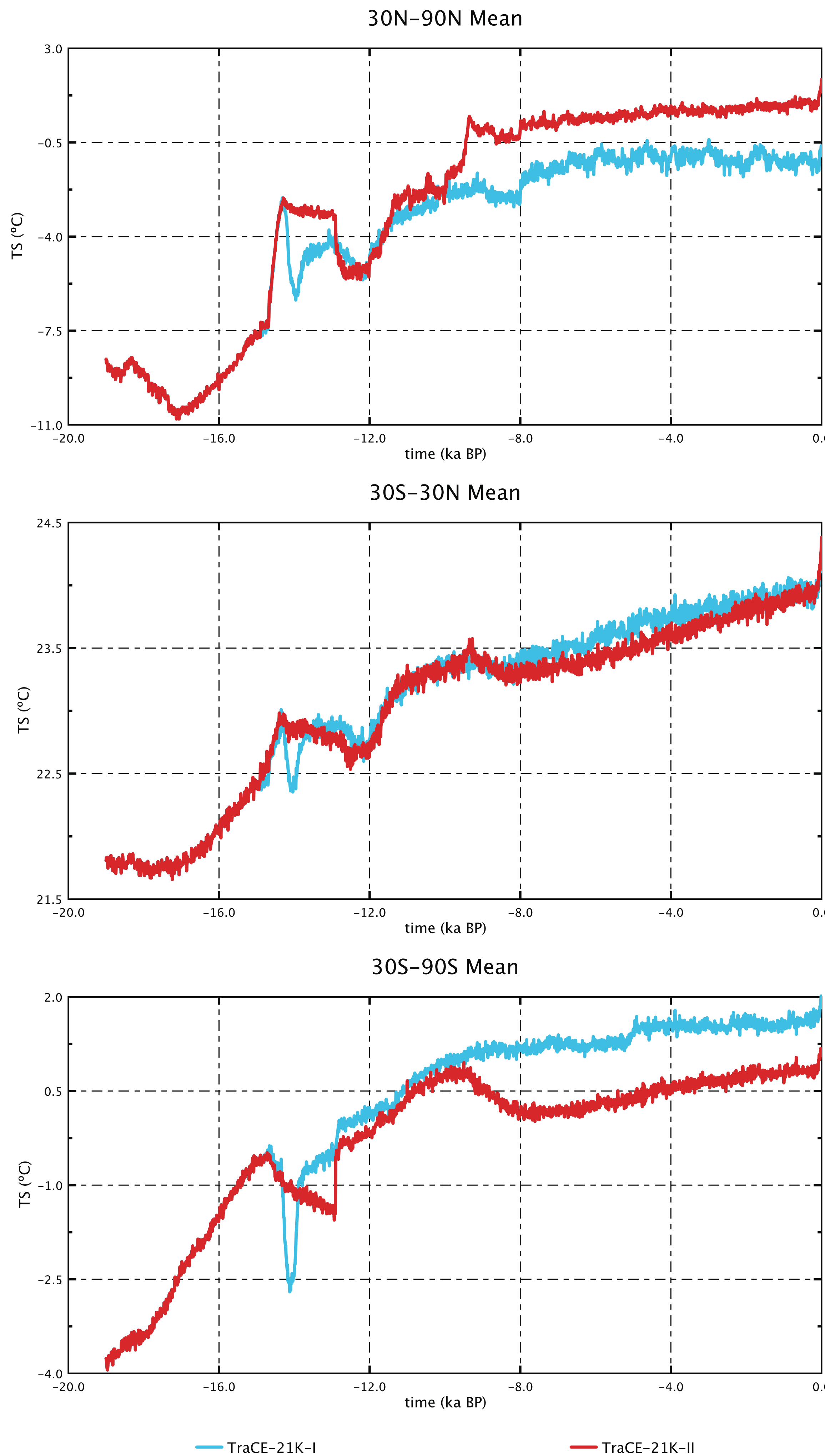
30N–90N Mean
TS (ºC)
3.0
-0.5
-4.0
-7.5
-11.0
−20.0
−16.0
−12.0
−8.0
−4.0
0.0
time (ka BP)
30S–30N Mean
TS (ºC)
24.5
23.5
22.5
21.5
−20.0
−16.0
−12.0
−8.0
−4.0
0.0
time (ka BP)
30S–90S Mean
TS (ºC)
2.0
0.5
-1.0
-2.5
-4.0
−20.0
−16.0
−12.0
−8.0
−4.0
0.0
time (ka BP)
TraCE-21K-I
TraCE-21K-II

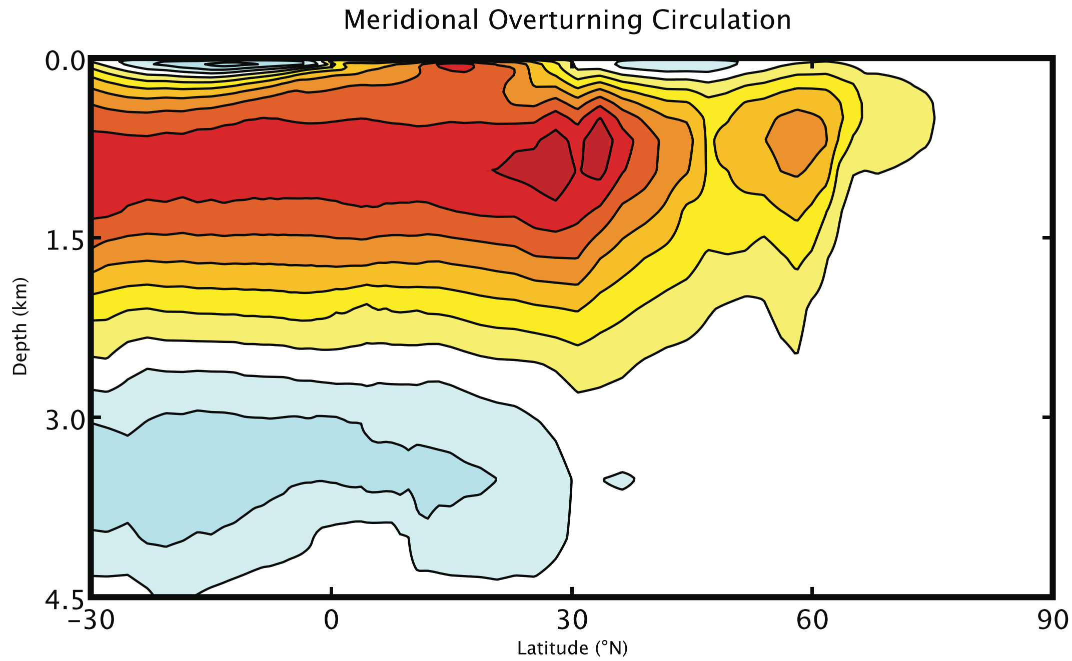
Meridional Overturning Circulation
0.0
1.5
3.0
4.5
Depth (km)
−30
0
30
60
90
Latitude (°N)

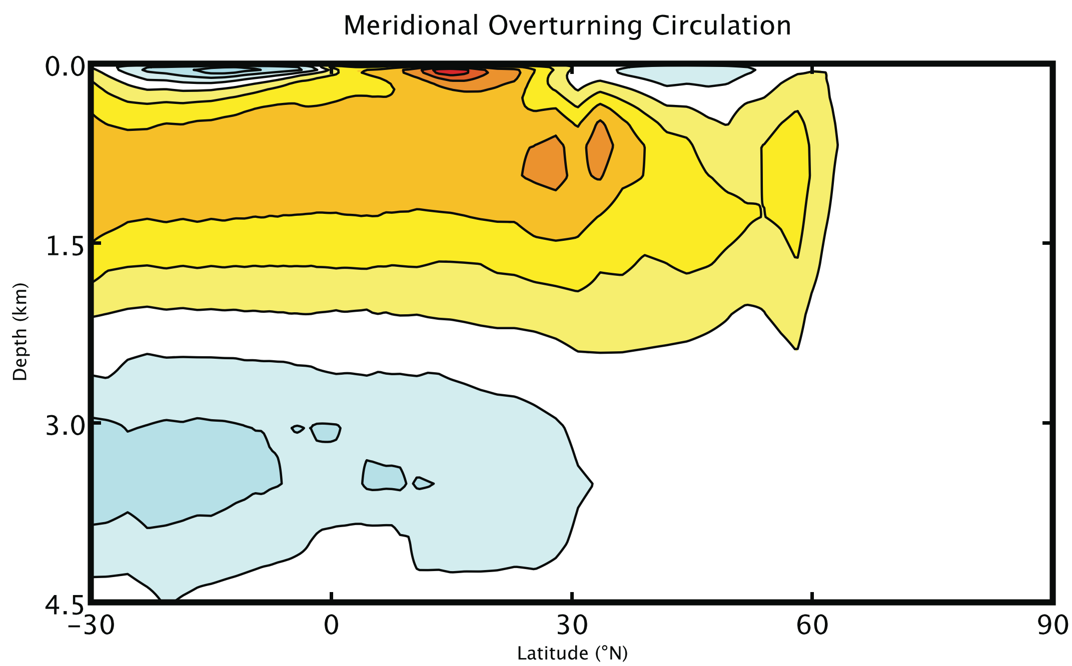
Meridional Overturning Circulation
0.0
1.5
3.0
4.5
Depth (km)
−30
0
30
60
90
Latitude (°N)

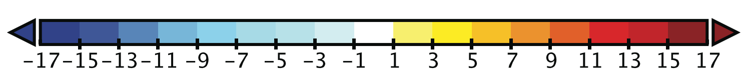
−17 −15 −13 −11 −9 −7 −5 −3 −1 1 3 5 7 9 11 13 15 17

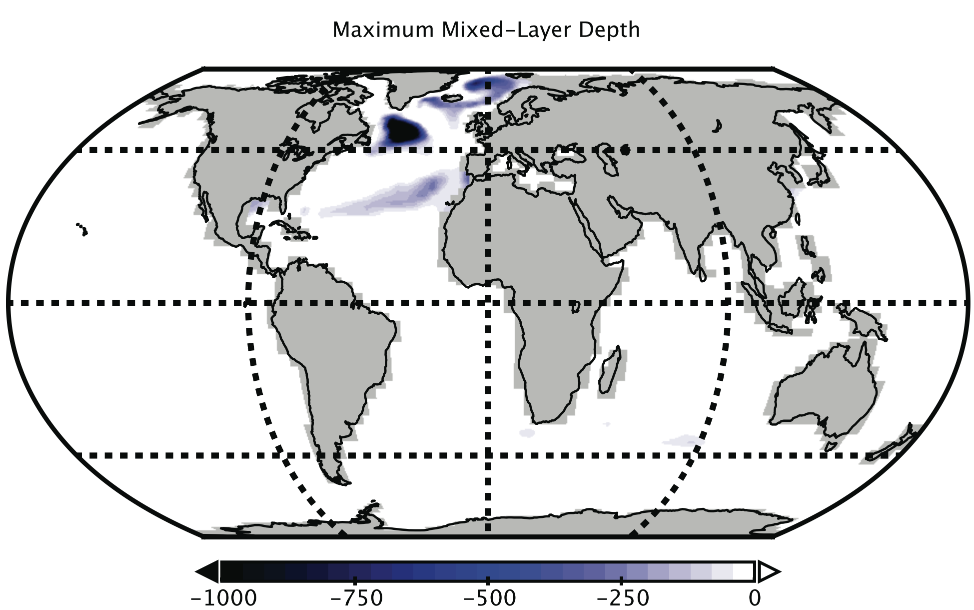
Maximum Mixed-Layer Depth
−1000
−750
−500
−250
0